J Solid State Electrochem (2002) 6: 183–187
DOI 10.1007/s100080100217

ORIGINAL PAPER

Michael Hyde · Andrew J. Saterlay · Shelley J. Wilkins
John S. Foord · Richard G. Compton · Frank Marken

Deposition and characterisation of a porous Sn(IV) semiconductor nanofilm on boron-doped diamond

Received: 5 October 2000 / Accepted: 30 March 2001 / Published online: 16 October 2001

Abstract Nanofilm deposits of a porous Sn(IV) oxide are formed by anodic electrodeposition on a polished boron-doped diamond electrode immersed in an aqueous Sn^{2+} solution. Mechanically and electrochemically stable deposits of 10–15 nm thickness are formed irrespective of the Sn^{2+} concentration and mass-transport enhancement by power ultrasound. Atomic force microscopy images indicate the presence of a smooth and noncrystalline film, which is stable under ambient conditions. n-type semiconducting characteristics are observed for the aqueous solution redox couples $Fe(CN)_6^{3-/4-}$ and $Ru(NH_3)_6^{3+/2+}$. However, preliminary results from voltammetric experiments indicate that the small and neutral organic molecule *N*,*N*,*N*′,*N*′-tetramethylphenylenediamine is able to diffuse through the porous film to undergo oxidation directly at the surface of the boron-doped diamond electrode.

Keywords Semiconductor · Porous film
Nanofilm · Boron-doped diamond · Voltammetry

Introduction

Thin film deposits containing Sn(IV) with tailored electronic properties are of considerable interest in various types of applications, such as gas sensors [1, 2, 3, 4], photovoltaic cells [5, 6], light-emitting devices [7], super capacitors [8], energy storage devices [9], electrocatalysis [10], and in corrosion protection [11]. Thin films containing Sn(IV) with indium as a conductivity enhancing dopant are in widespread use as transparent and highly conducting electrodes [12]. For the formation of thin film deposits starting from sols, spin-coating and casting is the procedure usually employed [13]; however, electrochemically formed thin films generated directly on metal surfaces by anodising [14] are also of considerable interest. Tin surface films formed during anodisation have been studied with respect to their photoelectrochemical properties [15, 16, 17]. Tin oxide films grown on foreign substrates, for example, by anodic precipitation from a solution phase, have received comparably little attention.

Sn(IV) oxide exhibits wide-band-gap n-type semiconducting behaviour [18] owing, for example, to oxygen vacancies [19, 20], and has been extensively characterised as electrode material in the past [21, 22]. Many studies addressing the behaviour of so-called "nanocrystalline" films of SnO_2 report similar characteristics, although the state of hydration and the solution pH may be anticipated to considerably influence the electrical characteristics. In a recent study [20] it was shown that a film of nanocrystalline tin oxide cast on a gold electrode effectively blocks the electrode for processes such as the reduction of $Fe(CN)_6^{3-}$, although, indications for ion and electron transport in the film were reported. Furthermore, the surface of SnO_2 is negatively charged over a wide pH range and this property has been exploited, for example, for the adsorption of cationic cyanine dye sensitisers on the surface.

Many types of metals exist in different redox states and allow anodic deposition on a conducting substrate during oxidation of an aqueous solution. Chemically reversible metal oxide deposition and stripping processes are very useful for applications in electroanalysis based on cathodic stripping voltammetry; recent examples including lead [23], manganese [24], and silver oxide [25]. For these three metals the deposition of oxides on boron-doped diamond materials results in well-defined and analytically useful voltammetric signals. In all three

M. Hyde · A.J. Saterlay · S.J. Wilkins · J.S. Foord
R.G. Compton
Physical & Theoretical Chemistry Laboratory,
Oxford University, South Parks Road, Oxford OX1 3QZ, UK

F. Marken (✉)
Department of Chemistry, Loughborough University,
Loughborough LE11 3TU, UK
E-mail: f.marken@lboro.ac.uk
Tel.: +44-1509-222551
Fax: +44-1509-223925

cases nucleation and growth of a particulate deposit was observed and characterised by atomic force microscopy (AFM). In contrast to oxidic deposits of Mn, Pb, and Ag, studies on Sn(IV) oxide indicate that the deposit formed anodically is exceptionally electrochemically inert over a wide potential range [11] as well as being mechanically stable without showing any cathodic stripping characteristics.

In this study the type of deposit formed during the oxidation of aqueous Sn(II) at a boron-doped diamond substrate was investigated by voltammetric and AFM techniques. It is demonstrated that polished boron-doped diamond is an ideal substrate for the study of thin film deposits of nanometre dimensions owing to the electrochemical and mechanical properties of diamond, which allow the film to be deposited homogeneously, partially removed mechanically, and then detected easily on the basis of the morphology difference between deposit and bare diamond. Further, the type of deposit formed is shown to be very different compared to oxides of Pb or Ag deposited anodically on boron-doped diamond. The extremely thin Sn(IV)-containing film (10–15 nm thickness) is demonstrated to exhibit n-type semiconducting properties for charged redox reagents in aqueous solution, whereas small neutral organic molecules such as *N*,*N*,*N*′,*N*′-tetramethylphenylenediamine (TMPD) may diffuse through the porous material formed during the anodic deposition process to undergo electrolysis directly at the boron-doped diamond substrate.

Experimental

Reagents

Chemical reagents HNO_3, KCl, $K_4Fe(CN)_6$, $K_3Fe(CN)_6$, TMPD, $Ru(NH_3)_6Cl_3$, and $SnSO_4$ (all Aldrich) were obtained in the highest commercially available purity and were used without further purification. Filtered and demineralised water was taken from an ELGASTAT water purification system (Elga, High Wycombe, Bucks) with a resistivity of not less than 18 MΩcm.

Instrumentation

For electrochemical measurements an Autolab PGSTAT 20 system (Eco Chemie, Netherlands) was employed. A three-electrode electrochemical cell equipped with a platinum gauze counterelectrode, a saturated calomel reference electrode (SCE, Radiometer, Copenhagen), and a polished 5 mm×5 mm boron-doped diamond working electrode [26] (De Beers Industrial Diamond, UK, or Windsor Scientific, Slough, UK) were employed. For sonoelectrochemical experiments an ultrasound horn transducer system (Sonics & Materials, VCX400) with a 3-mm diameter horn (titanium alloy) was employed. The horn probe was electrically insulated and positioned "face-on" towards the working electrode [27] at a distance of about 10 mm unless stated otherwise. A constant ultrasound power of 150 Wcm^{-2} was applied. All the experiments were conducted under an inert atmosphere of argon (BOC) and at a temperature of 22 ± 2 °C.

AFM images were obtained with a Topometrix 2010 Discoverer system (Thermo Microscopes, Bicester, UK) in *z*-topography mode and with 4-Hz scan rate.

Results and discussion

The deposition of metal oxides from a solution of the metal cation in a reduced redox state is often possible by immersion of an electrode and by applying a sufficiently positive potential to convert the soluble material into insoluble material. This kind of process is facile and clean, especially on boron-doped diamond electrodes, which provide a wide potential window, thereby suppressing unwanted side reactions such as substrate surface oxidation and oxygen evolution. The formation of metal oxide deposits on boron-doped diamond substrates has been studied for Pb, Mn, and Ag oxides and is often governed by nucleation at active sites [28] and formation of a particulate deposit.

A Sn(IV) oxide containing material may be deposited by anodic polarisation of an electrode immersed in a Sn(II)-containing aqueous solution. Voltammetric responses for the oxidation of 0.1, 1, and 10 mM Sn^{2+} solutions in aqueous 0.1 M HNO_3 at a 0.25-cm^2 boron-doped diamond electrode obtained under silent and under ultrasound conditions are shown in Fig. 1a and b, respectively. At high concentrations of Sn^{2+} the voltammetric responses obtained in the presence and in the absence of ultrasound are virtually identical; therefore, no mass-transport effect occurs and the peak shape as well as the amount of Sn(IV) deposited are limited by the growth process rather than by transport in solution.

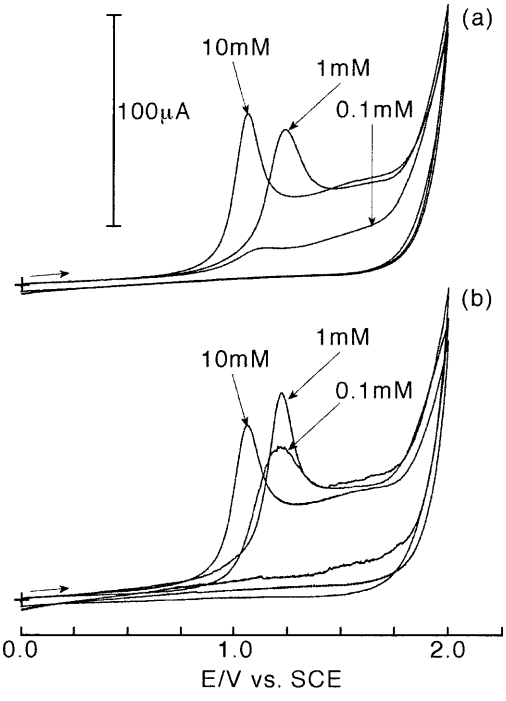

Fig. 1 Cyclic (staircase) voltammograms for the oxidation of 10, 1, and 0.1 mM Sn(II) sulfate in aqueous 0.1 M HNO_3 at a 5 mm×5 mm polished boron-doped diamond electrode **a** under silent conditions and **b** in the presence of ultrasound (150 Wcm^{-2}, 10-mm electrode-to-horn distance) obtained with a 1-mV step potential and a scan rate of 0.1 Vs^{-1}

In agreement with this, the magnitude of the current response is considerably smaller than that expected for a mass-transport-controlled process and integration over the current response allows the charge consumed in the deposition process to be determined. Assuming a two-electron oxidation, a total of 2 nmol of Sn(IV) was formed in the oxidation process and may be assumed to be present in form of a deposit.

At a concentration of 1 mM Sn^{2+} the deposition process occurs at a slightly more positive potential of $E_p = 1.25$ V versus SCE. A different peak shape can be observed on comparing the voltammetric signals for the deposition with and without ultrasound. At an even lower concentration of 0.1 mM Sn^{2+} the enhanced mass transport in the presence of ultrasound clearly has a dramatic effect in increasing the rate of deposition as shown in Fig. 1b compared to Fig. 1a. However, the amount of deposit formed during an exhaustive deposition process is essentially constant and independent of the Sn^{2+} concentration and mass-transport conditions. Experiments at concentrations of 10 and 1 μM Sn(II) also gave results consistent with Sn(IV) nanofilm deposition. Stripping of the Sn(IV) deposit was not observed even when the scan range for the reverse potential scan was extended to negative potentials. Only at a potential of about –1.5 V versus SCE was a cathodic current response detected (not shown); this was associated with the reduction and delamination of the film deposit; therefore, consistent with literature reports [11] and in contrast to the behaviour of many other metal oxide deposits, Sn(IV) film deposits formed in aqueous acidified solution are not suitable for cathodic stripping processes.

An AFM image of the film deposit formed under ultrasound conditions in a solution of 1 mM Sn^{2+} in 0.1 M HNO_3 is shown in Fig. 2. A very smooth and homogeneous film deposit is formed, which becomes apparent only after scratching the surface of the electrode with a razor blade. In Fig. 2 areas cleaned by the razor blade and areas with deposit can be clearly distinguished. The average thickness of the film varies between 10 and 15 nm (measured from the cross-section at several points). From the morphology of the film deposit and from the structure of the edges where material had been removed it is apparent that a predominantly amorphous material was formed.

It is interesting to evaluate the approximate density of the film deposit on the basis of the charge under the voltammetric peak and the volume of the deposit. By assuming the formation of SnO_2 (2 nmol) and a film volume of approximately 3.7×10^{-15} m^3 (from AFM measurements) a density of 0.8 gcm^{-3} is calculated. This value is much lower than the literature value of 6.9 gcm^{-3}; therefore, the deposited material must be porous or of different composition. The calculation for a hypothetical deposit of a strongly hydrated oxide [29] containing Sn(IV), $SnO_2(H_2O)_x$ with $x = 6$, gives a more reasonable result of 1.4 gcm^{-3} and perhaps an even higher water content is a more realistic representation of the composition of the deposit formed electrochemically.

Film deposits formed under silent conditions show very similar properties, although they seem to be even more difficult to detect by AFM techniques, presumably because of a softer, less dense structure. Depending on the magnitude of the force applied during the AFM measurement, the AFM tip appears to partially penetrate the softer film deposit formed in the absence of ultrasound. Sn(IV) oxide films deposited sonoelectrochemically onto boron-doped diamond and left for several days in air at room temperature did not suffer disintegration or loss of homogeneity; therefore, the film deposit appears to be stable with respect to dehydration and crystallisation under ambient conditions.

The adhesion and homogeneity of the Sn(IV) film formed on the boron-doped diamond substrate is very

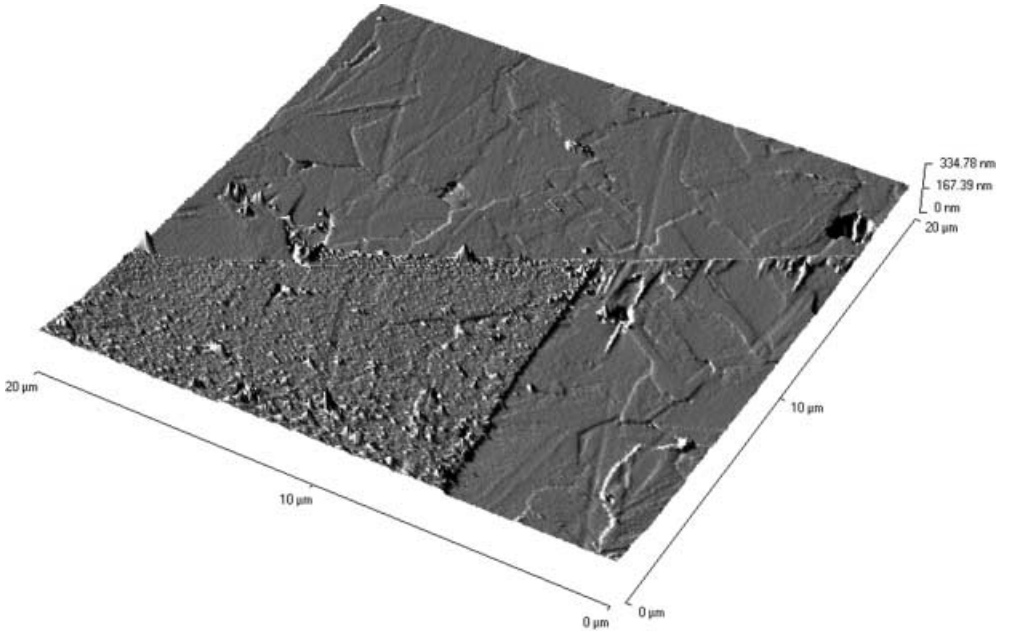

Fig. 2 Atomic force microscopy image of a polished boron-doped diamond electrode after deposition of a tin oxide film [1 mM Sn(II) sulfate in 0.1 M HNO_3, 150 Wcm^{-2} ultrasound] and after partial removal of the deposit with a razor blade

good and even under extreme conditions with very high ultrasound power (1-mm electrode-to-horn distance, 150-Wcm^2 ultrasound intensity) applied during deposition in a 1 mM Sn(II) solution in 0.1 M HNO_3 no loss of deposit was detected voltammetrically. This observation suggests that cavitational erosion has only a little effect on Sn(IV) oxide nanometre film deposits, whereas it has been shown recently that particulate deposits of PbO_2 are much more sensitive to the effects of power ultrasound [28]. Therefore, the Sn(IV) oxide deposit formed on boron-doped diamond could in future be employed in processes, for example, photoelectrochemical or electrocatalytic reactions, in the presence of power ultrasound [30].

The electronic properties of the Sn(IV) film deposited are closely related to those observed for other types of Sn(IV) containing deposits with n-type semiconducting characteristics. By depositing a Sn(IV) film onto the boron-doped diamond electrode (about 2 nmol), removing, rinsing the electrode surface with water, and reimmersing it in aqueous 0.1 M KCl containing 1 mM $Ru(NH_3)_6^{3+}$ it is possible to study the effect of the film on the reversible $Ru(NH_3)_6^{3+/2+}$ redox system (Eq. 1).

$$Ru(NH_3)_6^{3+}(aq) + e^- \rightleftarrows Ru(NH_3)_6^{2+}(aq) \quad (1)$$

Superimposed cyclic voltammograms obtained for the reduction of 1 mM $Ru(NH_3)_6^{3+}$ in 0.1 M KCl at a bare boron-doped diamond electrode and after deposition of the tin oxide film are shown in Fig. 3a. A dramatic change occurs from the reversible voltammogram detected at $E_{1/2} = -0.15$ V versus SCE in the absence of the film to an irreversible response detected at $E_p = -0.49$ V versus SCE in the presence of the film. No sign of a corresponding oxidation process after reversal of the scan direction is observed, which is in agreement with a semiconducting film becoming negatively conducting at a flat band potential of approximately $E_{fb} = -0.4$ V versus SCE. This value is in agreement with flat band potentials for Sn(IV) oxide at pH 7 reported in the literature [31, 32].

Cyclic voltammograms obtained for the reduction of 1 mM $Fe(CN)_6^{3-}$ in aqueous 0.1 M KCl at a bare boron-doped diamond electrode and at a tin oxide film are shown in Fig. 3b (Eq. 2).

$$Fe(CN)_6^{3-}(aq) + e^- \rightleftarrows Fe(CN)_6^{4-}(aq) \quad (2)$$

Consistent with the results for $Ru(NH_3)_6^{3+}$ and with the observations by Wang and Wang [20] a reversible voltammetric response with $E_{1/2} = 0.22$ V versus SCE is transformed into an irreversible wave at $E_p = -0.40$ V versus SCE in the presence of the tin oxide film. The voltammetric response for the reduction of ferricyanide occurs at a potential about 0.5 V more negative.

In contrast to the results observed for charged redox systems such as aqueous $Ru(NH_3)^{3+}$ and $Fe(CN)_6^{3-}$, neutral redox reagents of sufficiently small molecular dimension may be expected to penetrate into the porous tin oxide deposit. This can be demonstrated for the

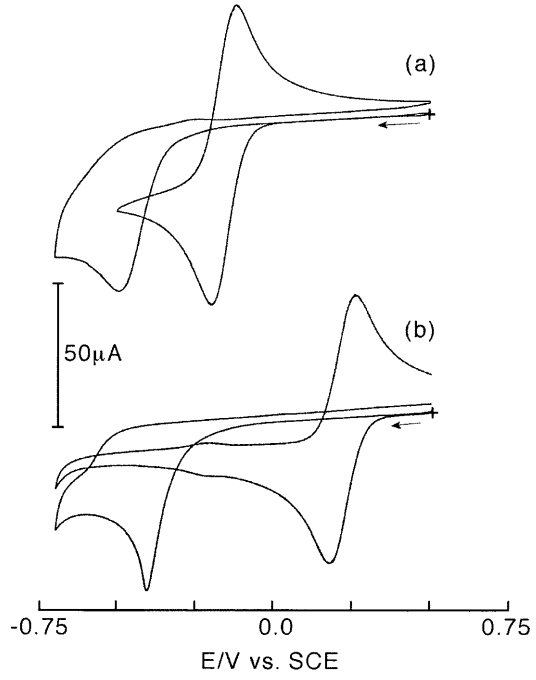

Fig. 3 Cyclic (staircase) voltammograms **a** for the reduction of 1 mM $Ru(NH_3)_6^{3+}$ in aqueous 0.1 M KCl and **b** for the reduction of 1 mM $Fe(CN)_6^{3-}$ in aqueous 0.1 M KCl at a 5 mm×5 mm polished boron-doped diamond electrode before and after deposition of a tin oxide nanofilm deposit [deposition in 1 mM Sn(II) sulfate in 0.1 M HNO_3]; step potential 1 mV and scan rate 0.1 Vs^{-1}

oxidation of TMPD, which is known to undergo two reversible one-electron oxidation processes (Eqs. 3, 4) in aqueous 0.1 M KCl [33].

$$TMPD(aq) \rightleftarrows TMPD^+(aq) + e^- \quad (3)$$

$$TMPD^+(aq) \rightleftarrows TMPD^{2+}(aq) + e^- \quad (4)$$

Cyclic voltammograms for the oxidation of 1 mM TMPD in 0.1 M KCl at a bare boron-doped diamond electrode and in the presence of the tin oxide layer are shown superimposed in Fig. 4. At a bare boron-doped diamond electrode two well-defined oxidation processes at $E_{1/2,I} = 0.02$ V versus SCE and at $E_{1/2,II} = 0.46$ V versus SCE are detected. More complex voltammetric characteristics have been observed only for a boron-doped diamond electrode material with lower doping level [33]. In the presence of the tin oxide film two oxidation waves, at approximately 0.34 and 0.59 V versus SCE, are detected in the first cycle of the cyclic voltammogram. No reduction response associated with the oxidation is detected down to potentials of –0.5 V versus SCE and the oxidation response diminishes in subsequent cycles. Only at a potential of $E_p = -0.83$ V versus SCE can the reduction of the oxidised form of TMPD be detected and after passing through this cathodic response the oxidation process can be detected again.

These results obtained by cyclic voltammetry may be interpreted in terms of the initially neutral TMPD

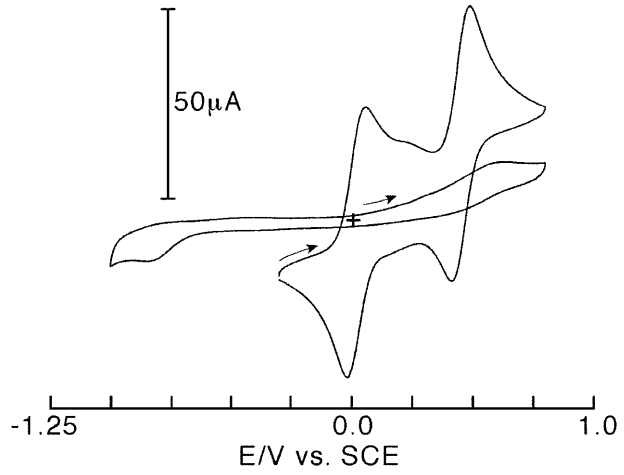

Fig. 4 Cyclic (staircase) voltammograms for the oxidation of 1 mM *N*, *N*, *N*′, *N*′-tetramethylphenylenediamine in aqueous 0.1 M KCl at a 5 mm×5 mm polished boron-doped diamond electrode before and after deposition of a nanofilm deposit of tin oxide [deposition in 1 mM Sn(II) sulfate in 0.1 M HNO_3]; second cycle shown, step potential 1 mV and scan rate 0.1 Vs^{-1}

diffusing into the porous tin oxide film and reaching the boron-doped diamond electrode surface. Within the pores of the film the neutral TMPD is oxidised to the mono- and dicationic forms, which can be assumed to strongly adsorb to the tin oxide. After reversal of the scan direction it is necessary to go beyond the flat-band potential to reduce the $TMPD^{n+}$ back into the neutral state, which then can be detected again during oxidation. This surprisingly complex interpretation of the voltammetric characteristics of the nanofilm Sn(IV) oxide deposit is consistent with reports [20] of ion conductivity and with the observation of a relatively low film density.

Conclusions

It has been shown that a mechanically stable Sn(IV) oxide nanofilm is formed by oxidation of Sn^{2+} in aqueous solution at a boron-doped diamond electrode substrate. This nanofilm deposit was characterised by AFM and voltammetric experiments. The voltammetric responses observed in the presence of aqueous redox systems suggest semiconducting behaviour and complete blocking for charged redox systems such as $Fe(CN)_6^{3-}$ and $Ru(NH_3)_6^{3+}$. However, for the case of TMPD oxidation in aqueous solution it was shown that neutral organic molecules may penetrate the porous nanofilm and can be detected undergoing redox processes directly at the boron-doped diamond substrate. Further interesting electrochemical characteristics may be expected for the case when a neutral organic reagent is oxidised within the film to form a neutral product, which may then be predicted to escape by diffusion through the nanofilm deposit.

Acknowledgements F.M. thanks the Royal Society for the award of a University Research Fellowship. The Nuffield foundation and New College, Oxford, are gratefully acknowledged for generous support of this project. De Beers Industrial Diamond Ltd. is gratefully acknowledged for providing boron-doped diamond electrodes.

References

1. Zhihong J, Zhou HJ, Jin ZL, Savinell RF, Liu CC (1998) Sens Actuators B 52:188
2. Varghese OK, Malhotra LK (1998) Sens Actuators B 53:19
3. Jayaraman V, Gnanasekar KI, Prabhu E, Gnanasekaran T, Periaswami G (1999) Sens Actuators B 55:147
4. Shimizu Y, Yamaguchi K, Fukunaga K, Takao Y, Hyodo T, Egashira M (1999) J Electrochem Soc 146:1222
5. Heimer TA, Heilweil EJ, Bignozzi CA, Meyer GJ (2000) J Phys Chem A 104:4256
6. Liu D, Fessenden RW, Hug GL, Kamat PV (1997) J Phys Chem B 101:2583
7. Kim H, Gilmore CM, Pique A, Horwitz JS, Mattoussi H, Murata H, Kafafi ZH, Chrisey DB (1999) J Appl Phys 86:6451
8. Li N, Martin CR, Scrosati B (2000) Electrochem Solid State Lett 3:316
9. Idota Y, Kubota T, Matsufuji A, Maekawa Y, Miyasaki T (1997) Science 276:1395
10. Grimm JH, Bessarabov DG, Simon U, Sanderson RD (2000) J Appl Electrochem 30:293
11. Galus Z (1973) In: Bard AJ (ed) Encyclopedia of electrochemistry of the elements. Dekker, New York, p 223
12. Obeng YS, Bard AJ (1991) Langmuir 7:195
13. Lemon BI, Hupp JT (1997) J Phys Chem B 101:2426
14. Metikos-Hukovic M, Omanovic S, Jukic A (1999) Electrochim Acta 45:97, and references therein
15. Zhang L, Gao EQ, Yang MZ, Qiao XB, Hao YZ, Cai SM, Meng FS, Tian H (1999) Acta Phys Chim Sin 15:293
16. Zhang L, Yang MZ, Qiao XB, Hao YZ, Wang YQ, Cai SM (1999) Acta Chim Sin 57:1129
17. Barazzouk S, Lee H, Hotchandani S, Kamat PV (2000) J Phys Chem B 104:3616
18. Moina CA, Varela FE, Hernandez LF, Ybarra GO, Vilche JR (1997) J Electroanal Chem 427:189
19. Messias FR, Scalvi LVA, Li MS, Santilli CV, Pulcinelli SH (1999) Radiat Eff Defects Solids 150:391
20. Wang WY, Wang CM (2000) J Chin Chem Soc 47:405
21. Morrison SR (1980) Electrochemistry at semiconductor and oxidized metal electrodes. Plenum, New York
22. Pleskov YV (1990) Solar energy conversion. Springer, Berlin Heidelberg New York
23. Saterlay AJ, Agra-Gutierrez C, Taylor MP, Marken F, Compton RG (1999) Electroanalysis 11:1083
24. Saterlay AJ, Foord JS, Compton RG (1999) Analyst 124:1791
25. Saterlay AJ, Wilkins SJ, Goeting CH, Foord JS, Compton RG, Marken F (2000) J Solid State Electrochem 4:383
26. Compton RG, Marken F, Goeting CH, McKeown RAJ, Foord JS, Scarsbrook G, Sussmann RS, Whitehead AJ (1998) Chem Commun 1961
27. Compton RG, Eklund JC, Marken F (1997) Electroanalysis 9:509
28. Saterlay AJ, Wilkins SJ, Holt KB, Foord JS, Compton RG, Marken F (2001) J Electrochem Soc 148:E66
29. Greenwood NN, Earnshaw A (1984) Chemistry of the elements. Pergamon, New York
30. Compton RG, Akkermans RP, Coles BA, Marken F (1997) Ultrason Sonochem 4:223
31. Biesmans G, Van der Auweraer M, Cathry C, Meerschaut D, De Schryver FC, Storck W, Willig F (1991) J Phys Chem 95:3771
32. Metikoshukovic M, Seruga M, Ferina S (1992) Phys Chem Chem Phys 96:799
33. Marken F, Compton RG, Goeting CH, Foord JS, Bull SD, Davies SG (2001) J Solid State Electrochem 5:8